On the importance of interplanetary magnetic field $|B_y|$ on polar cap patch formation

Q.-H. Zhang,[1] B.-C. Zhang,[1] R.-Y. Liu,[1] M. W. Dunlop,[2] M. Lockwood,[2,3] J. Moen,[4] H.-G. Yang,[1] H.-Q. Hu,[1] Z.-J. Hu,[1] S.-L. Liu,[1] I. W. McCrea,[2] and M. Lester[5]

Received 14 November 2010; revised 21 January 2011; accepted 21 February 2011; published 11 May 2011.

[1] A number of poleward moving events were observed between 1130 and 1300 UT on 11 February 2004, during periods of southward interplanetary magnetic field (IMF), while the steerable antenna of the European Incoherent Scatter (EISCAT) Svalbard radar (ESR) and the Tromsø VHF radar pointed nearly northward at low elevation. In this interval, simultaneous SuperDARN CUTLASS Finland radar measurements showed poleward moving radar aurora forms (PMRAFs) which appeared very similar to the density enhancements observed by the ESR northward pointing antenna. These events appeared quasiperiodically with a period of about 10 min. Comparing the observations from the above three radars, it is inferred that there is an almost one-to-one correspondence between the poleward moving plasma concentration enhancements (PMPCEs) observed by the ESR and the VHF radar and the PMRAFs measured by the CUTLASS Finland radar. These observations are consistent with the interpretation that the polar cap patch material was generated by photoionization at subauroral latitudes and that the plasma was structured by bursts of magnetopause reconnection giving access to the polar cap. There is clear evidence that plasma structuring into patches was dependent on the variability in IMF $|B_y|$. The duration of these events implies that the average evolution time of the newly opened flux tubes from the subauroral region to the polar cap was about 33 min.

Citation: Zhang, Q.-H., et al. (2011), On the importance of interplanetary magnetic field $|B_y|$ on polar cap patch formation, *J. Geophys. Res.*, *116*, A05308, doi:10.1029/2010JA016287.

1. Introduction

[2] Magnetic reconnection is a fundamental plasma process, resulting in energy and momentum transfer from the solar wind to the magnetosphere. Reconnection was first discussed in terms of a steady process by *Dungey* [1961] and was later discovered to show an independently intermittent and spatially limited nature by *Haerendel et al.* [1978] and then by *Russell and Elphic* [1978] on the dayside magnetopause. The magnetic signatures arising from the passage of bundles of reconnected flux nearby a spacecraft were named flux transfer events (FTEs) by *Russell and Elphic* [1978]. The early work of *Elphic et al.* [1990] demonstrated that ionospheric flow bursts measured by European Incoherent Scatter (EISCAT) were associated with FTEs observed by the International Sun-Earth Explorer (ISEE) and the first magnetically conjugate measurements of an FTE by Equator-S and of ionospheric flow bursts by SuperDARN were presented by *Neudegg et al.* [1999]. Poleward moving events or poleward moving flow channels, observed by the EISCAT radar, are widely accepted to be associated with bursts in the rate of dayside magnetopause reconnection generating new open flux [e.g., *Davis and Lockwood*, 1996; *Lockwood et al.*, 1993a, 2000, 2001a, 2001b, 2005a, 2005b; *Pitout et al.*, 2002; *Oksavik et al.*, 2004, 2005; *Rinne et al.*, 2010]. Poleward moving plasma concentration enhancements (sometimes called "polar cap patches") [*Davies et al.*, 2002] are frequently observed in the *F* region of the polar ionosphere during periods of southward interplanetary magnetic field (IMF), and are also thought to be associated with bursty reconnection [e.g., *Lockwood and Carlson*, 1992; *Carlson et al.*, 2002, 2004]. Poleward moving regions of backscatter or enhanced backscatter power, known as "poleward moving radar auroral forms" (PMRAFs), the radar counterpart of "poleward moving auroral forms" (PMAFs), are often also observed and are widely accepted to be another ionospheric signature of FTEs [e.g., *Sandholt et al.*, 1990; *Milan et al.*, 2000; *Wild et al.*, 2001; *Moen et al.*, 1995, 2001a, 2008a; *Zhang et al.*, 2008]. The east-west motion of these radar auroral forms depends on IMF B_y [*Sandholt et al.*, 1993; *Karlson et al.*, 1996; *Moen et al.*, 1999,

[1] SOA Key Laboratory for Polar Science, Polar Research Institute of China, Shanghai, China.
[2] SSTD, Rutherford-Appleton Laboratory, Chilton, UK.
[3] Space Environment Physics Group, Department of Meteorology, University of Reading, Reading, UK.
[4] Department of Physics, University of Oslo, Oslo, Norway.
[5] Department of Physics and Astronomy, University of Leicester, Leicester, UK.

0148-0227/11/2010JA016287

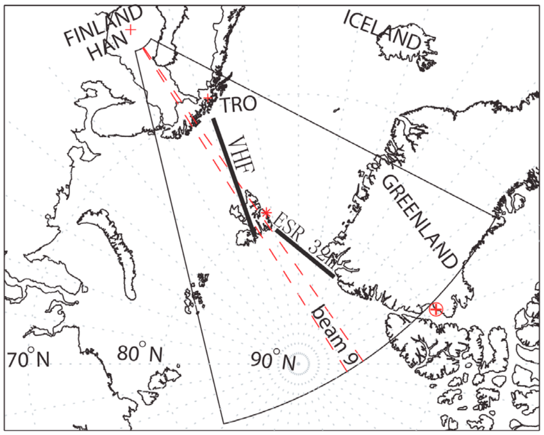

Figure 1. The lines of sight of the poleward looking low-elevation beam (32 m dish) of ESR (between 76° and 85° magnetic latitude) and the beam of the EISCAT VHF radar (between 68° and 80° magnetic latitude) are projected on a coast map (solid black lines). The field of view of the CUTLASS Finland radar (HAN) is presented as a "fan," together with the beam employed in this study, which is indicated by red dashed lines.

2001b]. *Pinnock et al.* [1995] and *Provan et al.* [1998] described the radar signatures of FTEs as "pulsed ionospheric flows" (PIFs), i.e., poleward moving regions of enhanced convection flow in the dayside auroral zone. Depending on the exact nature of the convection response to transient reconnection, either PMRAFs or PIFs, or both can be observed by the SuperDARN radars [e.g., *Milan et al.*, 2000; *Zhang et al.*, 2008; *Provan et al.*, 1998; *Wild et al.*, 2001, 2003]. The ionospheric flow direction is consistent with the motion of FTEs at the magnetopause [*Zhang et al.*, 2008, 2010]. *Zhang et al.* [2008] found that the flux tube motion, both measured and modeled from the inferred X line, qualitatively matches the clear velocity enhancements and the flow directions of ionospheric convections, measured simultaneously by the SuperDARN radar network in both hemispheres.

[3] Polar cap patches were defined by *Crowley* [1996] as islands of high-density ionospheric plasma surrounded by plasma of half the density or less. After formation by ionospheric cusp dynamics, the patches follow the convection pattern across the pole from day to night and are pulled into the nightside oval on exiting the polar cap [*Buchau et al.*, 1983; *Weber et al.*, 1984; *Lorentzen et al.*, 2004; *Moen et al.*, 2007]. While polar cap patches have been studied for over two decades, there remains no general agreement on which of the many proposed patch production mechanisms are important or dominant. The difficulty with patch segmentation is to explain the low-density regions between patches [*Lockwood et al.*, 2005b]. The mechanisms that have been suggested to segment the intake of cold solar EUV ionized plasma into the cusp throat can be divided into three families [*Lockwood et al.*, 2005b; *Oksavik et al.*, 2006; *Moen et al.*, 2006]: (1) IMF regulation of the cusp convection pattern, causing alternating intake of high- and low-density plasma [*Anderson et al.*, 1988; *Rodger et al.*, 1994; *Milan et al.*, 2002]; (2) plasma depletion within flow burst channels due to enhanced recombination associated with newly opened magnetic flux tubes [*Rodger et al.*, 1994; *Sojka et al.*, 1993; *Valladares et al.*, 1994; *Pitout and Blelly*, 2003; *Pitout et al.*, 2004]; and (3) plasma structuring by transient reconnection where the open closed boundary (OCB) leaps equatorward to a region of higher-density plasma, followed by poleward relaxation of that boundary carrying with it the high-density plasma accelerated into the polar flow [*Lockwood and Carlson*, 1992; *Lockwood et al.*, 2000; *Carlson et al.*, 2002, 2004, 2006]. *Sojka et al.* [1993] also suggested that the "tongue of ionization (TOI)" can provide a source of patches. The TOI is a region of dense daytime thermal plasma that is drawn from a sunlit subcusp region into the polar cap through the cusp region [*Knudsen*, 1974].

[4] *Moen et al.* [2008b] found that intake of high-density plasma material into the polar cap was independent of IMF B_y, but that the direction of the zonal movement of plasma depended on the IMF B_y component, giving rise to an MLT asymmetry of occurrence rate around magnetic noon. *Moen et al.* [2007] concluded that statistically patches populate the dawn and the dusk convections cells equally.

[5] In this paper, we present a close comparison of poleward moving events, including both PMPCEs (or polar cap patches) and PMRAFs, resulting from the bursts of magnetopause reconnection, as observed by the EISCAT Svalbard radar (ESR) [*Wannberg et al.*, 1997], the EISCAT VHF radar [*Rishbeth and van Eyken*, 1993] and the Co-operative UK, Twin Located Auroral Sounding System (CUTLASS) [*Milan et al.*, 1997; *Lester et al.*, 2004] Finland radar. By combining the three data sets, we attempt to reveal the plasma transportation process in the polar ionosphere which is associated with the motion of the newly opened flux tubes generated by magnetopause reconnection.

2. Instrumentation

[6] The EISCAT Scientific Association has, among others, a two dish incoherent scatter radar system near Longyearbyen on Svalbard (see Figure 1), known as the EISCAT Svalbard radar, or the ESR. One dish (a 32 m parabolic antenna) is fully steerable toward any direction, and the other (a 42 m parabolic antenna) is fixed, pointing along the local magnetic field line. The EISCAT Tromsø VHF radar, located near Tromsø on the Scandinavian mainland, is steerable only in elevation. Data from the two dishes of the ESR and from the EISCAT VHF radar are used in this study.

[7] The CUTLASS radars are the easternmost pair of SuperDARN radars [*Greenwald et al.*, 1995; *Chisham et al.*, 2007] in the Northern Hemisphere. The SuperDARN radars normally measure the line-of-sight (l-o-s) Doppler velocity, spectral width, and the backscatter power from ionospheric plasma irregularities in 16 adjacent beam directions separated by 3.24° in azimuth. A full normal scan is completed either in 1 or 2 min, depending on the integration period along each beam, and covers 52° in azimuth and over 3000 km in range with a resolution of 45 km. The two CUTLASS radars have been upgraded such that two experimental modes can be run simultaneously, the so-called "stereo" capability [*Lester et al.*, 2004]. One of the CUTLASS radars located at Hankasalmi, Finland (62.3° N, 26.6° E) has a fan-shaped field of view covering the magnetic latitudes between 65° and 90° and including the look directions of the EISCAT

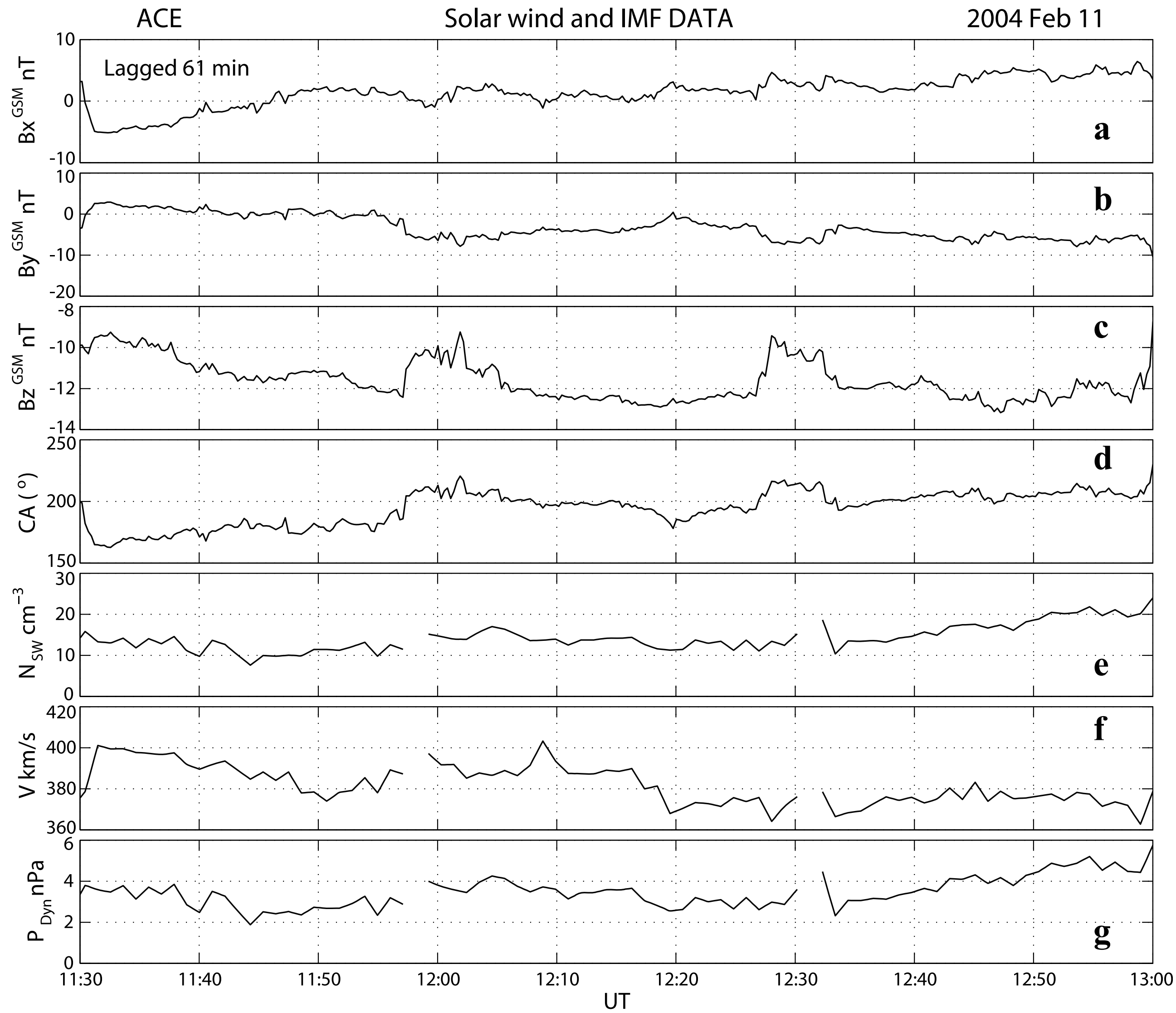

Figure 2. An overview of the solar wind and IMF conditions measured by the ACE satellite. Parameters shown: the GSM IMF components (a) B_x, (b) B_y, and (c) B_z; (d) the IMF clock angle (CA); (e) the solar wind plasma number density (N_{SW}); (f) the solar wind speed (V); and (g) the solar wind dynamic pressure (P_{dyn}).

VHF radar and the ESR (see Figure 1). Data from the CUTLASS Finland radar are also used here.

[8] The ACE satellite is in a halo orbit around the L1 Lagrange point and monitors the upstream solar wind and IMF conditions. Around 1200 UT on 11 February 2004, the ACE spacecraft was located at about (221.2, −32.4, 9.8) R_E in GSM coordinates. Solar wind data with 64s resolution from the Solar Wind Experiment [*McComas et al.*, 1998] and IMF data with 16s resolution from the Magnetometer instrument [*Smith et al.*, 1998] onboard the ACE spacecraft are used in this study.

3. Observations

3.1. Upstream Solar Wind and IMF Conditions

[9] Figure 2 presents an overview of the solar wind and IMF conditions measured by the ACE satellite. Parameters shown are the IMF components (in the GSM frame of reference) of B_x, B_y, B_z, the IMF clock angle, the solar wind plasma number density, the solar wind speed, and the solar wind dynamic pressure. The data have all been lagged by 61 min (this time delay is calculated using the method of *Liou et al.* [1998]) in order to take into account the propagation of solar wind/IMF structure from the spacecraft to magnetopause. During the whole interval, the IMF B_z component was always negative with values varying between −9 and −13 nT (see Figure 2c), while the B_y was slightly positive before 1154 UT (lagged time), and turned negative after that (see Figure 2b), so that the IMF clock angle varied from 160° to 220° (see Figure 2d), favoring a high reconnection rate. The solar wind density varied between about 8 and 23 cm^{-3} (see Figure 2e), while the solar wind velocity varied between 363 and 402 km/s (see Figure 2f), resulting in a prevailing solar wind dynamic pressure in the range 2.0–5.6 nPa (see Figure 2g).

3.2. ESR and VHF Radar Observations

[10] On 11 February 2004, the ESR 32 m dish was pointing nearly toward geomagnetic north (azimuth 336°), at low elevation (30°). The beam of the EISCAT VHF radar, operating at ~224 MHz, was also directed northward at low elevation, with a geographic azimuth of 359.45° and an elevation of 30°. The poleward looking low-elevation beam (32 m dish) of the ESR (covering the range between 76° and 85° magnetic latitude) and the beam of the EISCAT VHF radar (between 68° and 80° magnetic latitude) are indicated by the solid black lines in Figure 1, and allow us to monitor the plasma transportation in polar ionosphere from the subauroral region to the polar cap, in a configuration which provides something close to a single look direction. All the radars used alternating code measurement techniques to provide profiles of electron density, electron and ion temperature, and ion velocity along the line of sight.

[11] Figure 3 presents 2 min postintegrations of the ESR observations between 1130 and 1300 UT (about 1400 to 1530 Magnetic Local Time (MLT)) on 11 February 2004. Figure 3a presents observations of the electron density, the electron temperature, the ion temperature, and the line-of-sight ion velocity from the low-elevation northward directed ESR dish. The postintegrated data are shown as a function of magnetic latitude between 76° and 85° and the observations cover the altitude range from about 100 to 620 km. The density measurements indicated a series of high-density plasma regions (so-called poleward moving plasma concentration enhancements, PMPCEs or polar cap patches), moving along the beam to higher latitudes. These are highlighted by the black solid lines and marked as numbers 1–7. In these events, the plasma concentration (Ne) had a maximum density of about $3 \cdot 10^{11}$ cm^{-3} between 79° and 84° geomagnetic latitude (see the first panel of Figure 3a). These events appeared quasiperiodically with a period of about 10 min, which is consistent with the recurrence rate of less than 10 min reported by *Davies et al.* [2002]. It is worth noting that the events 4 and 5 were not real patches according to the requirement for a factor 2 enhancement above the background density, as defined by *Crowley* [1996]. The plasma gradients between these seven enhancements appeared to be regulated by IMF $|B_y|$, with the smallest gradient occurring when IMF B_y was near zero. We will discuss the effects of IMF B_y variation on the patch formation mechanism in further detail in section 4. The electron temperature decreased in these patches, highlighted by the black dashed lines in the same places as those in the above panel (see the second panel of Figure 3a). Although the ion temperature also showed enhancements (see the third panel of Figure 3a) and the plasma flow had clear poleward components between 1130 UT and 1300 UT (see the fourth panel of Figure 3a, where positive represents flow away from the radar), there were no clear plasma flow channels associated with the polar cap patches. This is not necessarily surprising, however, bearing in mind that the ESR is located in the polar cap where the convection pattern would be expected to show the combined effect resulting from the tailward motion of a number of separate flux tubes (FTEs) with different velocities. With the assumption that the poleward phase motion of the patches was roughly constant in speed [*Lockwood et al.*, 2001a; *Pitout et al.*, 2002], the black straight line can be mapped back to a magnetic latitude of about 76°, representing the time at which the patches would have passed the location of the field-aligned ESR beam, shown by the black vertical lines. Figure 3b presents the same parameters from the field-aligned ESR dish (azimuth 181°, elevation 81.6°), as a function of altitude between 100 to 800 km. The electron density was high and well structured in the *F* region, whereas the region below about 200 km appeared to be almost empty (i.e., dark blue). This suggests that the high-density plasma was simply transported through the *F* region with the poleward plasma flow. Around the black vertical lines, the electron density showed clear enhancements, which matched well to the events seen propagating poleward in the low-elevation beam, while the ion temperatures were also enhanced, indicating convection electric field enhancements [e.g., *Pitout et al.*, 2002]. The electron temperature decreased at the time that the patches passed through the field-aligned beam, consistent with previous observations of high electron density and low electron temperature in the polar cap patches reported by *Lockwood et al.* [2000, 2005a, 2005b] and *Moen et al.* [2004].

[12] In order to investigate the source and formation mechanism of these polar cap patches, we also checked the low-latitude observations from the EISCAT VHF radar. Figure 4 shows simultaneous observations of the electron density, the electron temperature, the ion temperature, and the line-of-sight ion velocity over the 67°–76° magnetic latitude range, made by the VHF radar. The open-closed boundary (OCB), shown by the black dashed line in the second panel of Figure 4, corresponds to the high electron temperature edge [*Doe et al.*, 2001; *Moen et al.*, 2004]. The OCB can be seen to have extended progressively equatorward, as the polar cap expanded due to magnetopause reconnection. Before about 1150 UT, the electron density appeared smooth and relatively high between about 70°–73° magnetic latitude (at an altitude between about 200–300 km), while the region poleward of the OCB showed very low electron density and high electron temperature at that time. After 1150 UT, the highest densities were apparently pushed equatorward as the OCB extended due to reconnection, and the electron density also began to show clear poleward moving plasma concentration enhancements (PMPCEs, see the first panel of Figure 4), highlighted by the black solid lines, together with transitory enhancements in the ion temperature (strong Joule heating). These suggest that the boundary carried the high-density plasma with it and accelerated it into the polar flow, corresponding to the expected response of the motion of the newly opened flux tubes (FTEs) generated by magnetopause reconnection [*Davis and Lockwood*, 1996; *Lockwood et al.*, 2000, 2001a, 2001b].

[13] The PMPCEs observed by the EISCAT VHF radar began about 8 min later than those measured by the ESR, either because these initial events only originated above 76° magnetic latitude or alternatively because bursty reconnection did not take place in the afternoon sector under the prevailing conditions of dominant southward IMF with a weak positive B_y component before 1150 UT. Although the ion velocity measured by the VHF radar showed clear poleward flows with velocities reaching about 800–1000 m/s, there were only a few clear separated flow channels associated with these poleward moving events. This might also be because of the combined effect resulting from mixing the tailward motion of several separate flux tubes (FTEs) with different velocities. It is worth noting that the electron

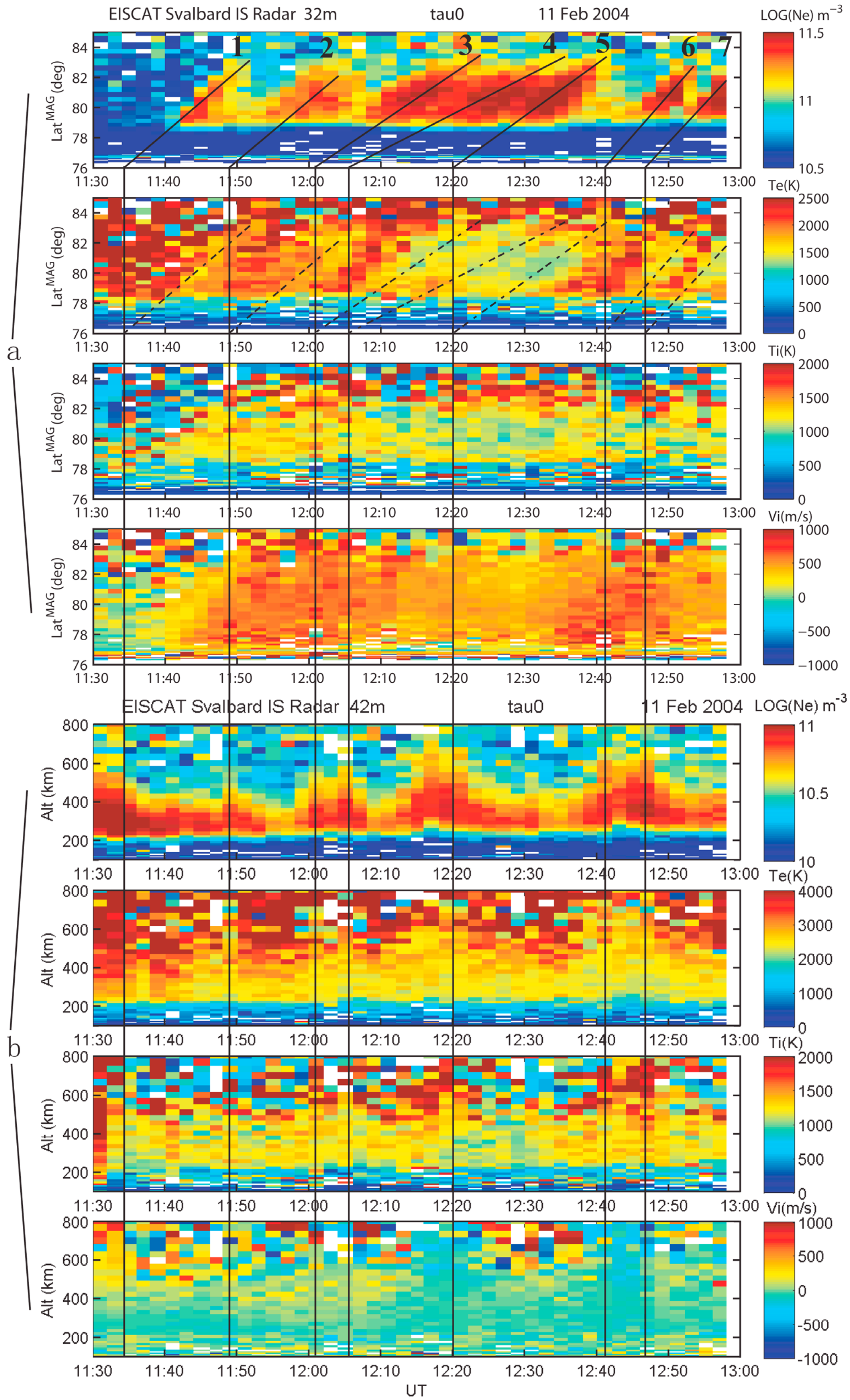

Figure 3. Plasma parameters observed by the northward directed ESR dish and the field-aligned dish on 11 February 2004: electron density (Ne), electron temperature (Te), ion temperature (Ti), and line-of-sight velocity (Vi, positive away from the radar) as a function of time and (a) magnetic latitude (Lat^{MAG}) or (b) altitude (Alt).

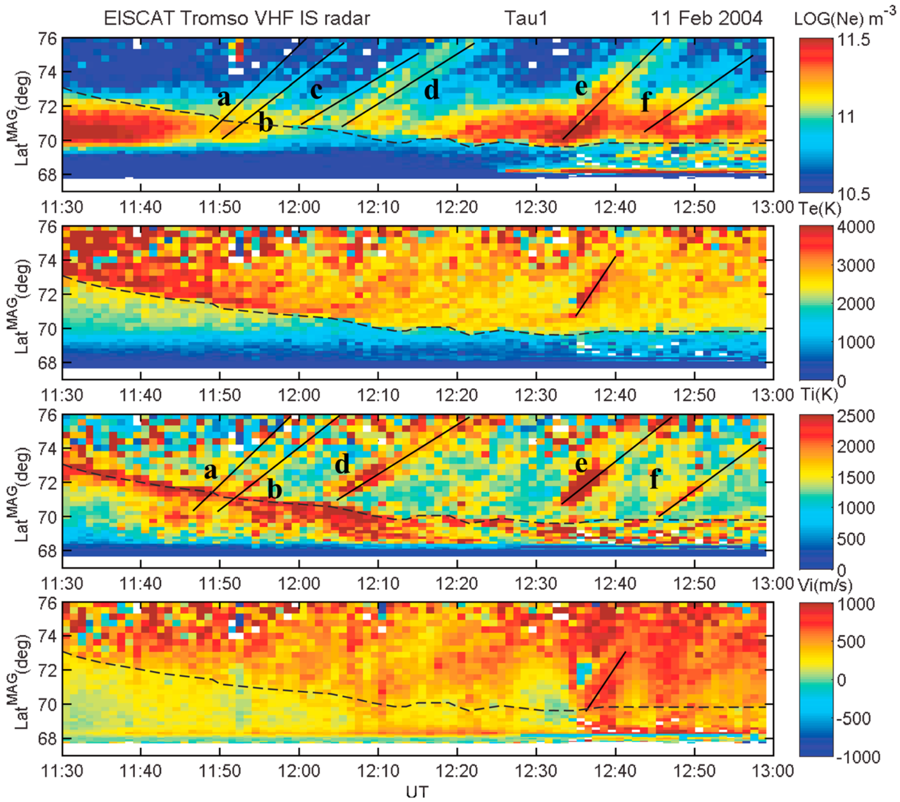

Figure 4. Simultaneous observations of electron density, electron temperature, ion temperature, and line-of-sight ion velocity over the 67°–76° range made by the EISCAT VHF radar between 1130 and 1300 UT on 11 February 2004.

densities in events e and f were higher than those in events a–d. This might be because a tongue of ionization (TOI) was moving across the line of sight of the VHF radar along the ionospheric convection streamlines, increasing the background electron density after 1215 UT. Detailed comparison and analysis of the formation mechanism for these events will be given in section 4.

3.3. CUTLASS Finland Radar Observations

[14] During the interval of interest, the CUTLASS Finland radar was running an experimental mode on channel B described in detail by *Karhunen et al.* [2006], with the normal scan, described above, on channel A. Only data from channel A are discussed in this paper. The backscatter power, line-of-sight (l-o-s) Doppler velocity, and spectral width observed by the CUTLASS Finland radar are used to examine the poleward moving events observed by the ESR and the VHF radar. The field of view of the CUTLASS Finland radar is presented as a "fan" in Figure 1, with the beam employed in this study indicated by the red dashed lines.

[15] Figure 5 shows the backscatter power, the l-o-s Doppler velocity and the Doppler spectral measured by the CUTLASS Finland SuperDARN radar during the period 1130–1300 UT on 11 February 2004. In Figure 5a, the backscatter power shows that there were 9 clear PMRAFs, marked by the black solid bias lines and numbered by i–ix. These PMRAFs were distributed between 75° and 81° magnetic latitude which covered the middle part of the look direction of the EISCAT VHF radar and the ESR (see Figure 1). These events also appeared quasiperiodically with a period of about 8 min, roughly consistent with the period of the enhanced plasma densities observed by the ESR and the EISCAT VHF radar. All of these events can be shown to correspond to the poleward moving events observed by the ESR or the VHF radar. We will discuss these in some detail later in section 4. The l-o-s velocity shows that the ionospheric convection was consistently antisunward (see Figure 5b) except for the ground scatter in gray, and that there were several PIFs associated with these PMRAFs. These observations are roughly consistent with the results reported by *Wild et al.* [2001, 2003]. The high spectral width values below about 76° suggest cusp-like features (see Figure 5c), and provide further evidence that the EISCAT VHF radar is unlikely to have seen poleward moving events before 1150 UT, since the events would have been initiated poleward of 76° magnetic latitude, even if reconnection had been taking place at this time under conditions of dominate southward IMF with a weak positive B_y component.

4. Discussion

[16] In Figure 4, we noted that the electron density was smooth and relatively high between about 70°–73° magnetic latitude before about 1150 UT, suggesting that the radar was observing cold solar EUV ionized plasma on closed field lines [*Foster*, 1984; *Moen et al.*, 2006]. This is consistent

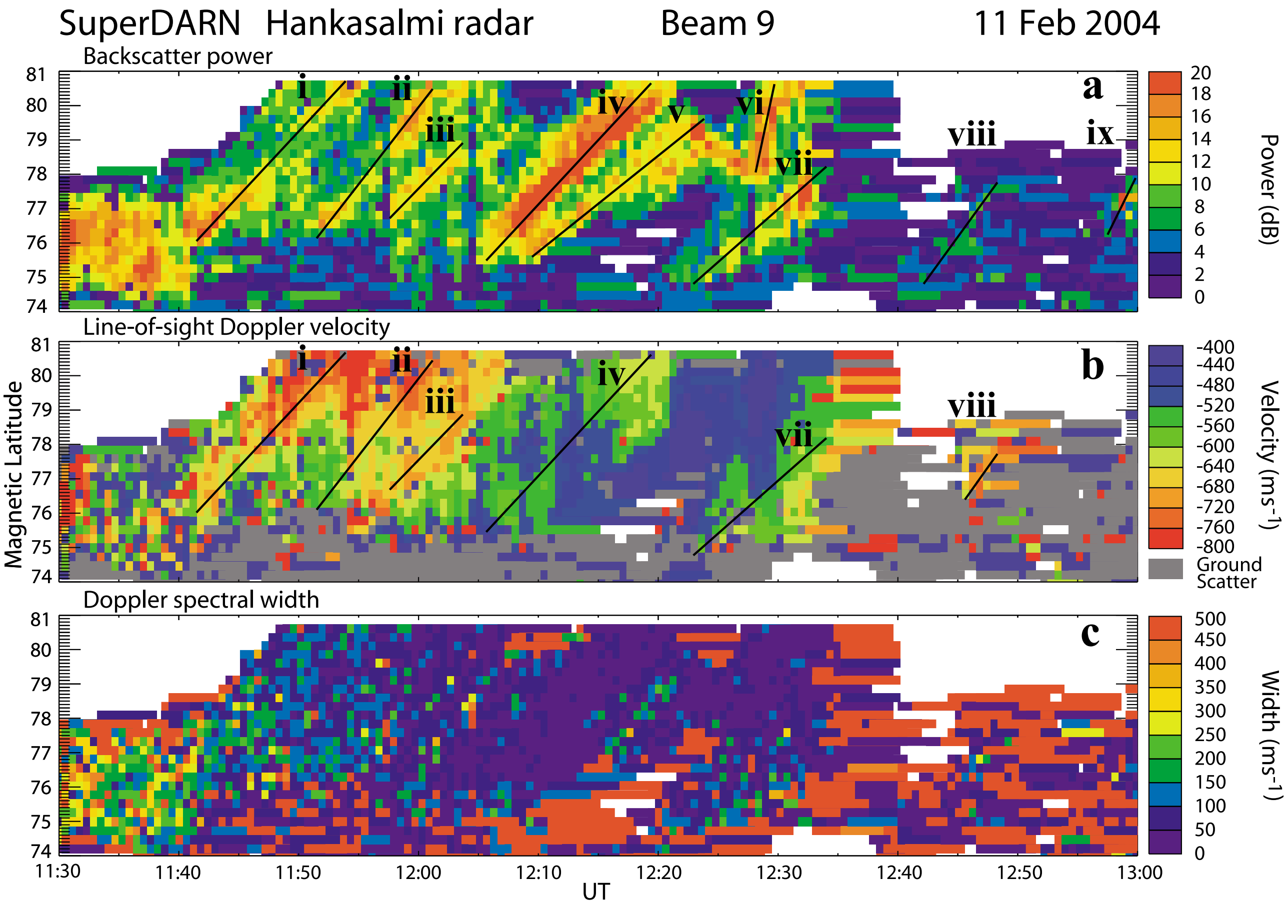

Figure 5. (a) Backscatter power, (b) l-o-s Doppler velocity, and (c) Doppler spectral width measured by the CUTLASS Finland SuperDARN radar during the period 1130–1300 UT on 11 February 2004.

with the OCB being located close to a gradient in plasma density, with solar EUV ionized plasma on the equatorward side, as previously reported by *Lockwood and Carlson* [1992] and by *Carlson et al.* [2006]. Poleward of OCB before about 1150 UT, the electron density appeared to be very low and the electron temperature is very high, possibly suggesting that there is an electron density trough, in which the *F* region ionospheric plasma convected along the ionospheric convection streamlines from the nightside and were heated immediately when they traveled through the sunlit region.

[17] In order to confirm the above inferences, we have also checked the ionospheric convection observed by the SuperDARN radars, which have a large field of view to monitor the plasma transportation over almost the entire polar ionosphere. Figure 6 shows the 2 min averaged flow maps at 1130 UT and 1200 UT for the Northern Hemisphere from the CUTLASS radars (HAN and PYK), the Stokkseyri radar (STO) and the Goose Bay radar (GBR) on geomagnetic grids with coastlines and the terminator projected on the altitude of 100 km (downloaded from http://superdarn.jhuapl.edu/). Grayed concentric circles indicate lines of constant magnetic latitude in 10° increments. Noon is located at the top of each pattern. The lagged IMF in the IMF Y-Z plane is shown as a black line in the top right of each panel, where the circle represents 10 nT. The field of view of the CUTLASS radars (HAN and PYK), the Stokkseyri radar (STO) and the Goose Bay radar (GBR) are shown as fans. During the interval of interest, all of these radars provided good data coverage. These measurements were combined using the "Map Potential" fitting technique [*Ruohoniemi and Baker*, 1998] to produce maps of large-scale ionospheric convection. The beam of CUTLASS Finland radar employed in this study is indicated by red dashed lines. The lines of sight of the poleward looking ESR and the EISCAT VHF radar are presented by solid black lines (similar as that in Figure 1).

[18] In Figure 6a, the day-night terminator shows that sunlight was able reach to altitudes above 100 km below about 73°, around the line of sight of the EISCAT VHF radar. This implies that the smooth and concentrated structure in the electron density observed by the VHF radar between about 70°–73° (at an altitude between about 200–300 km) before 1150 UT (see the first panel of Figure 4) was generated by the solar EUV ionization. Above about 74°, there were clear westward flows, reaching about 1500 m/s, corresponding to the possible location of the electron density trough between 74° and 79° (the region poleward of the OCB) in the postnoon sector. The high-latitude ionospheric convection pattern depends upon the solar wind–magnetosphere coupling (i.e., pulsed magnetopause reconnections) and the variable IMF orientation. Under conditions of southward IMF, closed field lines are opened by reconnection near the

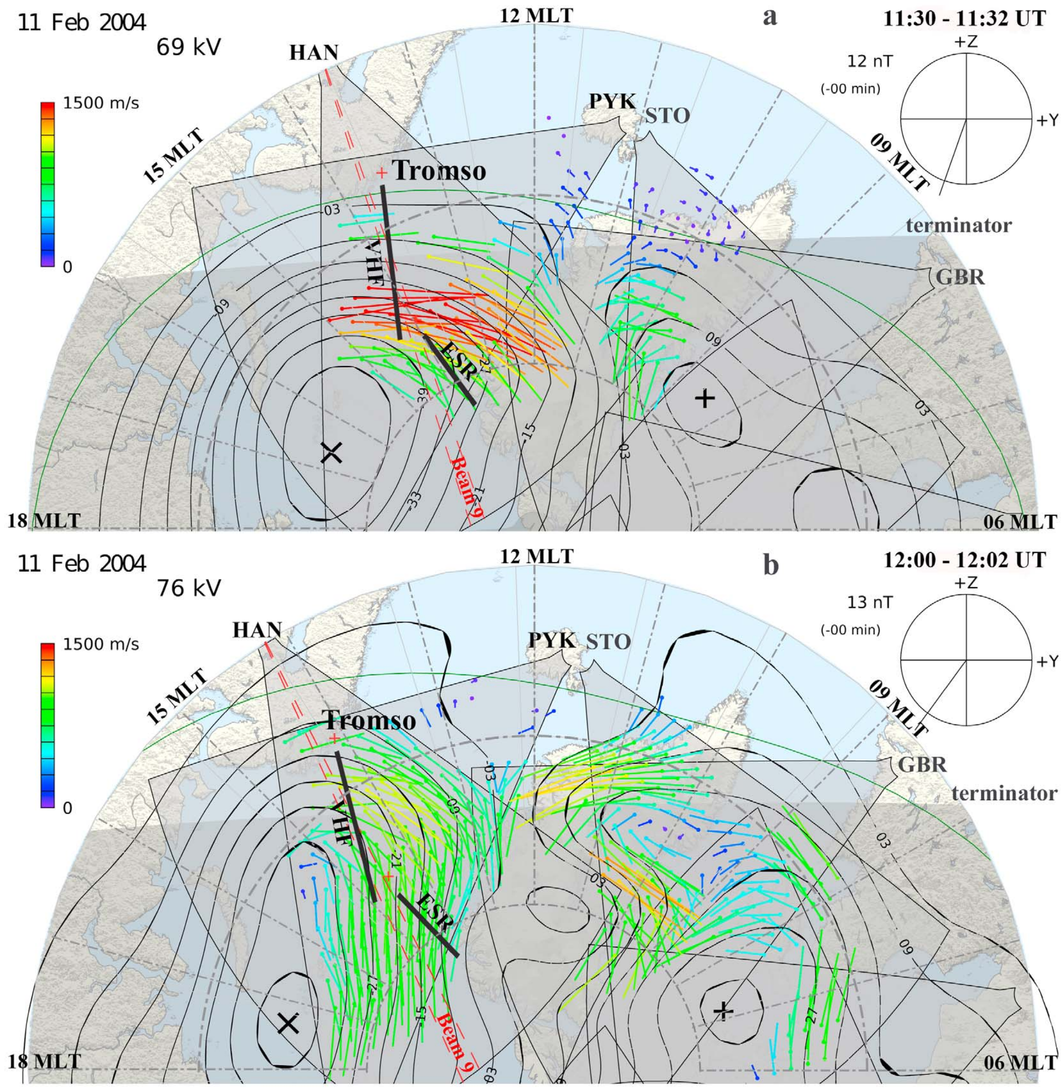

Figure 6. Streamlines and vectors of the ionospheric flows at (a) 1130 and (b) 1200 UT derived from the Northern Hemispheric SuperDARN velocity measurements shown on geomagnetic grids and a coast map with the terminator, obtained from the "map potential" algorithm. The fields of view of the CUTLASS radars (HAN and PYK), the Stokkseyri radar (STO), and the Goose Bay radar (GBR) are presented as fans. The beam of the CUTLASS Finland radar employed in this study is indicated by red dashed lines. The lines of sight of the poleward looking ESR and the EISCAT VHF radar are presented by solid black lines (similar to Figure 1). The direction and magnitude of the lagged IMF are indicated by the vector at the upper right-hand corner of each map.

equatorial magnetopause, which leads to the equatorward expansion of the convection pattern and the ionospheric flows being dragged antisunward with poleward flux tube motions. In Figure 6b, measured 30 min later, the convection pattern had extended equatorward and the ionospheric flows had turned mainly northward around the line of sight of the EISCAT VHF radar and the ESR. These observations confirm the OCB extension and put into context the associated poleward moving events observed by the ESR and the VHF radar.

[19] In order to discuss the source and formation mechanism of these poleward moving events, we compared the observations from the poleward looking beams of the ESR, the EISCAT VHF radar and the CUTLASS Finland radar by extracting the first panels of Figures 3, 4, and 5, and combining them together in Figure 7. Comparing Figure 7 (top and middle), we observe that the electron densities were much lower in the PMPCEs observed by the EISCAT VHF radar (at low latitude) than that in the polar cap patches measured by the ESR (at high latitude). Moreover, it seems as if the electron densities in the PMPCEs observed by the VHF radar are similar to the densities in the minima between the patches measured by the ESR. This suggests the possibility that the patches observed by the ESR were segmented by the less dense poleward moving events first observed by the EISCAT VHF radar, highlighted by the black dashed bias and vertical lines (see the first two panels of Figure 7). This conclusion is convincingly supported by

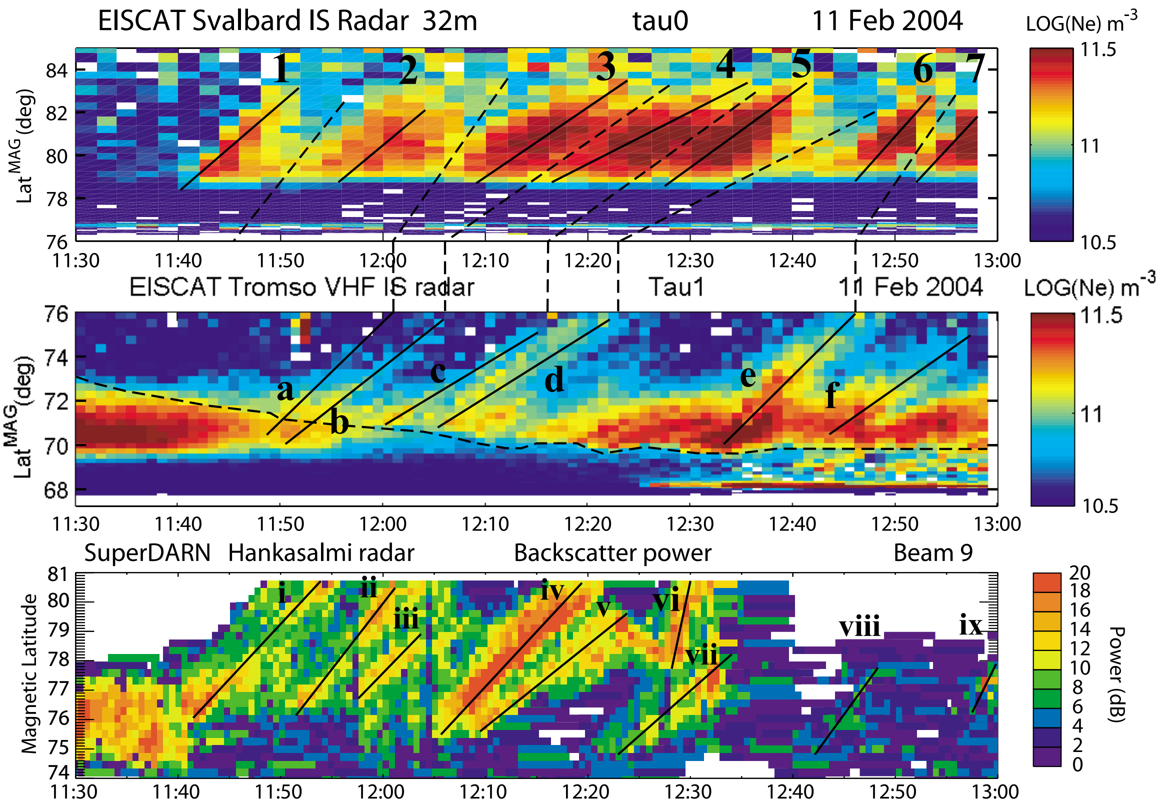

Figure 7. Electron density observed by the northward directed ESR dish and the EISCAT VHF radar (same as the top panels of Figures 3a and 4), together with the backscatter power measured by the CUTLASS Finland radar (same as Figure 5a) during the period 1130–1300 UT on 11 February 2004.

the dashed lines in the top panel of Figure 7, which show how the patches seen in the VHF data would have continued to propagate into the polar cap, had they maintained their meridional velocity.

[20] This would imply that some of these PMPCEs had moved from about 70° (the lower limit of Figure 7, middle) to 84° (the upper limit of Figure 7, top), in association with new open flux being generated by bursts in the magnetopause reconnection rate, and consistent with previous findings that most of the poleward moving patches with enhanced plasma concentration are associated such with a reconnection pulse [*Lockwood et al.*, 2005a, 2005b]. The average time taken by these events to move through the entire latitude range observed by the ESR and the VHF radar is about 33 min, which implies that the evolution time of the new open flux is about 33 min from subauroral region to the polar cap.

[21] The SuperDARN HF radars monitor the backscatter from high-latitude field-aligned ionospheric plasma density irregularities which act as tracers of the bulk plasma motion as they move under the influence of the convection electric field [*Milan et al.*, 1997]. A PMRAF, corresponding to a region of enhanced backscatter power which separates from a preexisting backscatter power enhancement and then moves poleward, is therefore expected to contain either more, or higher-amplitude, irregularities than the surrounding region. This implies that the PMRAFs observed by the CUTLASS Finland radar might not correspond exactly to the PMPCEs measured by the ESR and the VHF radar. Since PMRAFs are more likely to correspond to scatter from irregularities which form on the density gradients at the edges of PMPCEs [*Greenwald et al.*, 1995], it is possible that under some circumstances a PMPCE could give rise to a pair of PMRAFs, or that two closely spaced PMPCEs could be represented as one PMRAF in the backscatter power. However, because the PMRAFs observed by the CUTLASS Finland radars (Figure 7, bottom) were concentrated in the range 75°–81° magnetic latitude, we can be certain that they are associated with the PMPCEs observed by the ESR and VHF radars, and therefore with magnetopause reconnection. From Figure 7 (bottom), we suggest that event i (and ii) might correspond to polar cap patch 1 (and 2) (see Figure 7, top) combined with the electron density trough discussed above. Event iii (vii and ix) seems to correspond to patch a (d and 7), while events iv–vi appear to correspond to patches b–d and 3–5, respectively, and event viii to patches e and 6. It can hence be inferred that there is close correspondence between the polar cap patches observed by the EISCAT radars and the PMRAFs observed by the CUTLASS Finland radar, which is consistent with earlier results reported by *McCrea et al.* [2000] and *Lockwood et al.* [2000].

[22] From Figure 7, it can be inferred that the polar cap patches observed by the ESR were segmented by the poleward moving events observed by the EISCAT VHF radar. This confirms for the first time the mechanism of the patch formation which suggested that plasma structuring could occur due to transient reconnection in which the OCB leaps

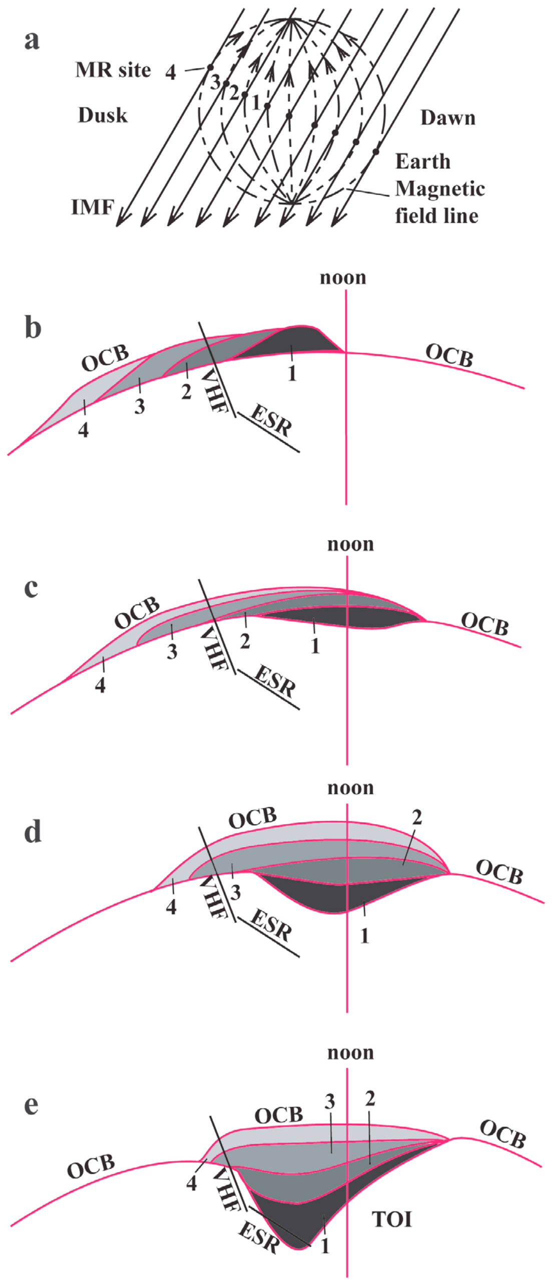

Figure 8. Schematic illustration of the magnetic reconnection between IMF and the Earth's magnetic field lines on the dayside magnetopause and of the theory of polar cap patch formation by *Lockwood et al.* [2000] for the Northern Hemisphere, during southward IMF with a negative IMF B_y component. The pulse of enhanced reconnection propagates through the afternoon sector away from 1200 MLT (noon, vertical line), opening the field lines: the darker shaded regions are opened earlier and at the smaller MLT.

equatorward to a region of higher-density plasma, followed by poleward relaxation of that boundary carrying with it the high-density plasma accelerated into the polar flow [*Lockwood and Carlson*, 1992; *Carlson et al.*, 2002, 2004, 2006; *Moen et al.*, 2006]. This mechanism is based on the concept that the active reconnection region expands rapidly away from noon during each event, as proposed by *Lockwood et al.* [1993b] and *Lockwood* [1994], as shown in Figure 8a. The dayside magnetopause magnetic reconnection (MR) X lines describe as an "S" shape (partly shown in Figure 8a) at the dayside magnetopause under a condition of IMF $B_z \approx B_y < 0$, which has been confirmed by the analysis of the shear angle between the magnetospheric and magnetosheath magnetic fields at the dayside magnetopause [*Moore et al.*, 2002] and by the statistical study of dayside reconnection observed by Cluster and Double Star [*Pu et al.*, 2007]. The shading of areas in Figures 8b–8e denotes the time sequence in which different regions are reconnected, the darker regions being reconnected earlier and closer to magnetic noon as the reconnection pulse propagates through the afternoon sector (see Figure 8a). Figures 8b–8e show the evolution of newly opened field lines, corresponding to reconnection sites 1–4 occurring in the afternoon sector, as they move westward under the magnetic curvature force [*Cowley et al.*, 1991; *Greenwald et al.*, 1990] before being assimilated into the polar cap by poleward motion [*Cowley and Lockwood*, 1992]. The black region 1, which reconnected near noon, represents the density peak of a patch, while the light gray region 4, originating furthest away from noon, will represent the minimum density between patches in a sequence [*Lockwood et al.*, 2000, 2005a, 2005b]. In Figures 8b–8e, the lines of sight of the ESR and the EISCAT VHF radar are presented as solid black lines. Before 1150 UT, the bursty reconnection might not take place in the afternoon sector under the prevailing conditions of dominant southward IMF with a weak positive B_y component (see Figure 2b), and in any case the EISCAT VHF radar was probably located too far south of the cusp to observe poleward moving features; instead observing the solar EUV ionized plasma in the region equatorward of OCB. After that time, reconnection began in the afternoon sector due to the IMF B_y turning negative, as illustrated in Figure 8a. The OCB expanded equatorward to a region of higher-density plasma (sunlit ionized plasma layer, see Figure 8b), followed by westward and poleward relaxation of that boundary, carrying with it the high-density plasma accelerated into the polar flow (see Figures 8c–8e) [*Lockwood and Carlson*, 1992; *Carlson et al.*, 2002, 2004, 2006; *Moen et al.*, 2006]. The process would eventually lead to the formation of a tongue of ionization (TOI). The EISCAT VHF radar would have been expected to observe only the lower-density part of the patch, which came from dusk sector, because the region observed by the radar was already located at about 1430 MLT (see Figures 8d and 8e), while the ESR would first have measured the higher-density part of the patch, which came from near noon, followed by the lower-density part (see Figure 8e). As illustrated in Figure 8, the reconnection pulse spans a longitudinal density gradient. If there was no such density gradient, there would be no patch formation, and the TOI would be a homogenous stream of plasma. A real patch, as defined by *Crowley* [1996], will be formed only in the case when the reconnection pulse spans a factor 2 in density gradient. For the sequence of poleward moving events presented in Figure 7 (top), the smallest plasma gradient occurred between events 4 and 5, under conditions of IMF $B_y \approx 0$ (see Figure 2b). The density variations in these events were not large enough for them to be true patches according to Crowley's definition. The formation of these events is, however, still consistent with the

Lockwood et al. [2005b] explanation of polar cap patch formation, as long as one assumes that the longitudinal extent of reconnection pulses 4 and 5 did not span a factor 2 density gradient. It should be stressed that this patch production mechanism does not require, but will also work for, IMF B_y polarity changes. The exact relationship between IMF variability and patch formation is obviously case dependent, as it simply depends on the plasma density gradient within the region of newly opened flux. An alternative way of expressing this is to say that the geometry of the reconnection site, controlled by IMF B_y, dictates the orientation of the OCB and the direction in which it will expand equatorward into regions of denser solar-produced ionization.

5. Conclusion

[23] We have presented a number of poleward moving events observed by the ESR, the VHF radar and the CUTLASS Finland radar between 1130 and 1300 UT on 11 February 2004, when the IMF was directed southward. These events appeared quasiperiodically with a period of about 10 min. Comparing the observations from these three radars, we inferred that there is close correspondence between the PMPECEs observed by the ESR and the EISCAT VHF radar, and the PMRAFs measured by the CUTLASS Finland radar. Our analysis indicates that the poleward moving events were generated by sunlit photoionization and convected into the polar cap when their field lines were opened by bursts of reconnection. Under this mechanism, true polar cap patches are formed only in the case when reconnection pulses span a factor 2 density gradient. Patch formation will therefore depend on the location as well as the MLT span of the X line relative to the high-density plasma source region bordering on the open-closed boundary, waiting to be grabbed by the next reconnection pulse. The observations provide the first evidence that patch formation may be very sensitive to IMF $|B_y|$. The durations of these events imply that the average evolution time of the newly open flux tube is about 33 min from the subauroral region to the polar cap.

[24] **Acknowledgments.** This work is supported by the Natural Science Foundation of Shanghai, China (grant 11ZR1441200), the National Natural Science Foundation of China (NSFC grants 40890164, 40604020, 40874082, and 41031064) and Ocean Public Welfare Scientific Research Project, State Oceanic Administration People's Republic of China (201005017). M. W. Dunlop is partly supported by Chinese Academy of Sciences (CAS) visiting Professorship for senior international scientists (grant 2009S1–54). M. Lester is supported by STFC grant ST/H002480/1. J. Moen is supported by the Norwegian Research Council and COST ES803. We acknowledge the NASA CDAWeb site for supplying us with the solar wind and IMF data from the ACE spacecraft.

[25] Robert Lysak thanks the reviewers for their assistance in evaluating this paper.

References

Anderson, D., J. Buchau, and R. Heelis (1988), Origin of density enhancements in the winter polar cap ionosphere, *Radio Sci.*, *23*(4), 513–519, doi:10.1029/RS023i004p00513.

Buchau, J., B. Reinisch, E. Weber, and J. Moore (1983), Structure and dynamics of the winter polar cap *F* region, *Radio Sci.*, *18*(6), 995–1010, doi:10.1029/RS018i006p00995.

Carlson, H. C., K. Oksavik, J. Moen, A. P. van Eyken, and P. Guio (2002), ESR mapping of polar-cap patches in the dark cusp, *Geophys. Res. Lett.*, *29*(10), 1386, doi:10.1029/2001GL014087.

Carlson, H. C., K. Oksavik, J. Moen, and T. Pedersen (2004), Ionospheric patch formation: Direct measurements of the origin of a polar cap patch, *Geophys. Res. Lett.*, *31*, L08806, doi:10.1029/2003GL018166.

Carlson, H. C., J. Moen, K. Oksavik, C. P. Nielsen, I. W. McCrea, T. R. Pedersen, and P. Gallop (2006), Direct observations of injection events of subauroral plasma into the polar cap, *Geophys. Res. Lett.*, *33*, L05103, doi:10.1029/2005GL025230.

Chisham, G., et al. (2007), A decade of the Super Dual Auroral Radar Network (SuperDARN): Scientific achievements, new techniques and future directions, *Surv. Geophys.*, *28*, 33–109, doi:10.1007/s10712-007-9017-8.

Cowley, S. W. H., and M. Lockwood (1992), Excitation and decay of solar wind-driven flows in the magnetosphere-ionosphere system, *Ann. Geophys.*, *10*, 103–115.

Cowley, S., J. Morelli, and M. Lockwood (1991), Dependence of convective flows and particle precipitation in the high-latitude dayside ionosphere on the X and Y components of the interplanetary magnetic field, *J. Geophys. Res.*, *96*, 5557–5564, doi:10.1029/90JA02063.

Crowley, G. (1996), Critical review of ionospheric patches and blobs, in *Review of Radio Science 1992–1996*, edited by W. R. Stone, pp. 619–648, Oxford Univ. Press, Oxford, U. K.

Davies, J. A., T. K. Yeoman, I. J. Rae, S. E. Milan, M. Lester, M. Lockwood, and A. McWilliams (2002), Ground-based observations of the auroral zone and polar cap ionospheric responses to dayside transient reconnection, *Ann. Geophys.*, *20*, 781–794, doi:10.5194/angeo-20-781-2002.

Davis, C. J., and M. Lockwood (1996), Predicted signatures of pulsed reconnection in ESR data, *Ann. Geophys.*, *14*, 1246–1256.

Doe, R. A., J. D. Kelly, and E. R. Sánchez (2001), Observations of persistent dayside *F* region electron temperature enhancements associated with soft magnetosheath-like precipitation, *J. Geophys. Res.*, *106*, 3615–3630, doi:10.1029/2000JA000186.

Dungey, J. W. (1961), Interplanetary magnetic field and the auroral zones, *Phys. Rev. Lett.*, *6*, 47–48, doi:10.1103/PhysRevLett.6.47.

Elphic, R. C., M. Lockwood, S. W. H. Cowley, and P. E. Sandholt (1990), Flux transfer events at the magnetopause and in the ionosphere, *Geophys. Res. Lett.*, *17*(12), 2241–2244, doi:10.1029/GL017i012p02241.

Foster, J. C. (1984), Ionospheric signatures of magnetospheric convection, *J. Geophys. Res.*, *89*, 855–865, doi:10.1029/JA089iA02p00855.

Greenwald, R. A., K. B. Baker, J. M. Ruohoniemi, J. R. Dudeney, M. Pinnock, N. Mattin, J. M. Leonard, and R. P. Lepping (1990), Simultaneous conjugate observations of dynamic variations in high-latitude dayside convection due to changes in IMF B_y, *J. Geophys. Res.*, *95*, 8057–8072, doi:10.1029/JA095iA06p08057.

Greenwald, R. A., et al. (1995), DARN/SuperDARN: A global view of the dynamics of high-latitude convection, *Space Sci. Rev.*, *71*, 761–796, doi:10.1007/BF00751350.

Haerendel, G., G. Paschmann, N. Sckopke, H. Rosenbauer, and P. Hedgecock (1978), The frontside boundary layer of the magnetosphere and the problem of reconnection, *J. Geophys. Res.*, *83*, 3195–3216, doi:10.1029/JA083iA07p03195.

Karhunen, T. J. T., N. F. Arnold, T. R. Robinson, and M. Lester (2006), Determination of the parameters of traveling ionospheric disturbances in the high-latitude ionosphere using CUTLASS coherent-scatter radars, *J. Atmos. Sol. Terr. Phys.*, *68*, 558–567, doi:10.1016/j.jastp.2005.03.021.

Karlson, K. A., M. Øieroset, J. Moen, and P. E. Sandholt (1996), A statistical study of flux transfer event signatures in the dayside aurora: The IMF B_y-related prenoon-postnoon asymmetry, *J. Geophys. Res.*, *101*, 59–68, doi:10.1029/95JA02590.

Knudsen, W. C. (1974), Magnetospheric convection and the high-latitude F_2 ionosphere, *J. Geophys. Res.*, *79*, 1046–1055, doi:10.1029/JA079i007p01046.

Lester, M., et al. (2004), Stereo CUTLASS—A new capability for the SuperDARN radars, *Ann. Geophys.*, *22*, 459–473, doi:10.5194/angeo-22-459-2004.

Liou, K., P. T. Newell, and C.-I. Meng (1998), Characteristics of the solar wind controlled auroral emissions, *J. Geophys. Res.*, *103*, 17,543–17,557.

Lockwood, M. (1994), Ionospheric signatures of pulsed magnetopause reconnection, in *Physical Signatures of Magnetopause Boundary Layer Processes*, *NATO ASI Ser., Ser. C*, vol. 425, edited by J. A. Holtet and A. Egeland, pp. 229–243, Kluwer Acad., Dordrecht, Netherlands.

Lockwood, M., and H. C. Carlson (1992), Production of polar cap electron density patches by transient magnetopause reconnection, *Geophys. Res. Lett.*, *19*(17), 1731–1734, doi:10.1029/92GL01993.

Lockwood, M., W. F. Denig, A. D. Farmer, V. N. Davda, S. W. H. Cowley, and H. Lühr (1993a), Ionospheric signatures of pulsed magnetic reconnection at the Earth's magnetopause, *Nature*, *361*, 424–428, doi:10.1038/361424a0.

Lockwood, M., J. Moen, S. W. H. Cowley, A. D. Farmer, U. P. Løvhaug, H. Lühr, and V. N. Davda (1993b), Variability of dayside convection and motions of the cusp/cleft aurora, *Geophys. Res. Lett.*, *20*(11), 1011–1014, doi:10.1029/93GL00846.

Lockwood, M., I. W. McCrea, S. E. Milan, J. Moen, J. C. Cerisier, and A. Thorolfsson (2000), Plasma structure within poleward-moving cusp-cleft auroral transients: EISCAT Svalbard radar observations and an explanation in terms of large local time extent of events, *Ann. Geophys.*, *18*, 1027–1042, doi:10.1007/s00585-000-1027-5.

Lockwood, M., et al. (2001a), Co-ordinated Cluster, ground-based instrumentation and low-altitude satellite observations of transient poleward-moving events in the ionosphere and in the tail lobe, *Ann. Geophys.*, *19*, 1589–1612, doi:10.5194/angeo-19-1589-2001.

Lockwood, M., et al. (2001b), Co-ordinated Cluster and ground-based instrument observations of transient changes in the magnetopause boundary layer during an interval of predominantly northward IMF: Relation to reconnection pulses and FTE signatures, *Ann. Geophys.*, *19*, 1613–1640, doi:10.5194/angeo-19-1613-2001.

Lockwood, M., J. Moen, A. P. van Eyken, J. A. Davies, K. Oksavik, and I. W. McCrea (2005a), Motion of the dayside polar cap boundary during substorm cycles: I. Observations of pulses in the magnetopause reconnection rate, *Ann. Geophys.*, *23*, 3495–3511, doi:10.5194/angeo-23-3495-2005.

Lockwood, M., J. A. Davies, J. Moen, A. P. van Eyken, K. Oksavik, I. W. McCrea, and M. Lester (2005b), Motion of the dayside polar cap boundary during substorm cycles: II. Generation of poleward-moving events and polar cap patches by pulses in the magnetopause reconnection rate, *Ann. Geophys.*, *23*, 3513–3532, doi:10.5194/angeo-23-3513-2005.

Lorentzen, D. A., N. Shumilov, and J. Moen (2004), Drifting airglow patches in relation to tail reconnection, *Geophys. Res. Lett.*, *31*, L02806, doi:10.1029/2003GL017785.

McComas, D. J., S. J. Bame, P. Barker, W. C. Feldman, J. L. Phillips, P. Riley, and J. W. Griffee (1998), Solar Wind Electron Proton Alpha Monitor (SWEPAM) for the Advanced Composition Explorer, *Space Sci. Rev.*, *86*, 563–612, doi:10.1023/A:1005040232597.

McCrea, I. W., M. Lockwood, J. Moen, F. Pitout, P. Eglitis, A. D. Aylward, J.-C. Cerisier, A. Thorolfssen, and S. E. Milan (2000), ESR and EISCAT observations of the response of the cusp and cleft to IMF orientation changes, *Ann. Geophys.*, *18*, 1009–1026, doi:10.1007/s00585-000-1009-7.

Milan, S. E., T. K. Yeoman, M. Lester, E. C. Thomas, and T. B. Jones (1997), Initial backscatter occurrence statistics from the CUTLASS HF radars, *Ann. Geophys.*, *15*, 703–718, doi:10.1007/s00585-997-0703-0.

Milan, S. E., M. Lester, S. W. H. Cowley, and M. Brittnacher (2000), Convection and auroral response to a southward turning of the IMF: Polar UVI, CUTLASS and IMAGE signatures of transient magnetic flux transfer at the magnetopause, *J. Geophys. Res.*, *105*, 15,741–15,756.

Milan, S. E., M. Lester, and T. K. Yeoman (2002), HF radar polar patch formation revisited: Summer and winter variations in dayside plasma structuring, *Ann. Geophys.*, *20*, 487–499, doi:10.5194/angeo-20-487-2002.

Moen, J., P. E. Sandholt, M. Lockwood, W. F. Denig, U. P. Løvhaug, B. Lybekk, A. Egeland, D. Opsvik, and E. Friis-Christensen (1995), Events of enhanced convection and related dayside auroral activity, *J. Geophys. Res.*, *100*, 23,917–23,934.

Moen, J., H. C. Carlson, and P. E. Sandholt (1999), Continuous observation of cusp auroral dynamics in response to an IMF BY polarity change, *Geophys. Res. Lett.*, *26*(9), 1243–1246, doi:10.1029/1999GL900224.

Moen, J., A. P. van Eyken, and H. C. Carlson (2001a), EISCAT Svalbard radar observations of ionospheric plasma dynamics in relation to dayside auroral transients, *J. Geophys. Res.*, *106*, 21,453–21,461, doi:10.1029/2000JA000378.

Moen, J., P. E. Sandholt, and A. Egeland (2001b), Pre- and post-noon asymmetry in dayside auroral activity and convection related to solar wind-magnetosphere interactions, *Adv. Space Res.*, *27*, 1363–1372, doi:10.1016/S0273-1177(01)00031-X.

Moen, J., M. Lockwood, K. Oksavik, H. C. Carlson, W. F. Denig, A. P. van Eyken, and I. W. McCrea (2004), The dynamics and relationships of precipitation, temperature and convection boundaries in the dayside auroral ionosphere, *Ann. Geophys.*, *22*, 1973–1987, doi:10.5194/angeo-22-1973-2004.

Moen, J., H. C. Carlson, K. Oksavik, C. P. Nielsen, S. E. Pryse, H. R. Middleton, I. W. McCrea, and P. Gallop (2006), EISCAT observations of plasma patches at sub-auroral cusp latitudes, *Ann. Geophys.*, *24*, 2363–2374, doi:10.5194/angeo-24-2363-2006.

Moen, J., N. Gulbrandsen, D. A. Lorentzen, and H. C. Carlson (2007), On the MLT distribution of *F* region polar cap patches at night, *Geophys. Res. Lett.*, *34*, L14113, doi:10.1029/2007GL029632.

Moen, J., Y. Rinne, H. C. Carlson, K. Oksavik, R. Fujii, and H. Opgenoorth (2008a), On the relationship between thin Birkeland current arcs and reversed flow channels in the winter cusp/cleft ionosphere, *J. Geophys. Res.*, *113*, A09220, doi:10.1029/2008JA013061.

Moen, J., X. C. Qiu, H. C. Carlson, R. Fujii, and I. W. McCrea (2008b), On the diurnal variability in F2-region plasma density above the EISCAT Svalbard radar, *Ann. Geophys.*, *26*, 2427–2433, doi:10.5194/angeo-26-2427-2008.

Moore, T. E., M.-C. Fok, and M. O. Chandler (2002), The dayside reconnection X line, *J. Geophys. Res.*, *107*(A10), 1332, doi:10.1029/2002JA009381.

Neudegg, D. A., et al. (1999), A flux transfer event observed at the magnetopause by the Equator-S spacecraft and in the ionosphere by the CUTLASS HF radar, *Ann. Geophys.*, *17*, 707–711, doi:10.1007/s00585-999-0707-z.

Oksavik, K., J. Moen, and H. C. Carlson (2004), High-resolution observations of the small-scale flow pattern associated with a poleward moving auroral form in the cusp, *Geophys. Res. Lett.*, *31*, L11807, doi:10.1029/2004GL019838.

Oksavik, K., J. Moen, H. C. Carlson, R. A. Greenwald, S. E. Milan, M. Lester, W. F. Denig, and R. J. Barnes (2005), Multi-instrument mapping of the small-scale flow dynamics related to a cusp auroral transient, *Ann. Geophys.*, *23*, 2657–2670, doi:10.5194/angeo-23-2657-2005.

Oksavik, K., J. M. Ruohoniemi, R. A. Greenwald, J. B. H. Baker, J. Moen, H. C. Carlson, T. K. Yeoman, and M. Lester (2006), Observations of isolated polar cap patches by the European Incoherent Scatter (EISCAT) Svalbard and Super Dual Auroral Radar Network (SuperDARN) Finland radars, *J. Geophys. Res.*, *111*, A05310, doi:10.1029/2005JA011400.

Pinnock, M., A. S. Rodger, J. R. Dudeney, F. Rich, and K. B. Baker (1995), High spatial and temporal resolution observations of the ionospheric cusp, *Ann. Geophys.*, *13*, 919–925, doi:10.1007/s00585-995-0919-9.

Pitout, F., and P. Blelly (2003), Electron density in the cusp ionosphere: Increase or depletion?, *Geophys. Res. Lett.*, *30*(14), 1726, doi:10.1029/2003GL017151.

Pitout, F., P. T. Newell, and S. C. Buchert (2002), Simultaneous high- and low-latitude reconnection: ESR and DMSP observations, *Ann. Geophys.*, *20*, 1311–1320, doi:10.5194/angeo-20-1311-2002.

Pitout, F., C. P. Escoubet, and E. A. Lucek (2004), Ionospheric plasma density structures associated with magnetopause motion: A case study using the Cluster spacecraft and the EISCAT Svalbard radar, *Ann. Geophys.*, *22*, 2369–2379, doi:10.5194/angeo-22-2369-2004.

Provan, G., T. K. Yeoman, and S. E. Milan (1998), CUTLASS Finland radar observations of the ionospheric signatures of flux transfer events and the resulting plasma flows, *Ann. Geophys.*, *16*, 1411–1422, doi:10.1007/s00585-998-1411-0.

Pu, Z. Y., et al. (2007), Global view of dayside magnetic reconnection with the dusk-dawn IMF orientation: A statistical study for Double Star and Cluster data, *Geophys. Res. Lett.*, *34*, L20101, doi:10.1029/2007GL030336.

Rinne, Y., J. Moen, H. C. Carlson, and M. R. Hairston (2010), Stratification of east-west plasma flow channels observed in the ionospheric cusp in response to IMF BY polarity changes, *Geophys. Res. Lett.*, *37*, L13102, doi:10.1029/2010GL043307.

Rishbeth, H., and A. P. van Eyken (1993), EISCAT: Early history and the first ten years of operation, *J. Atmos. Terr. Phys.*, *55*, 525–542, doi:10.1016/0021-9169(93)90002-G.

Rodger, A., M. Pinnock, J. Dudeney, K. Baker, and R. Greenwald (1994), A new mechanism for polar patch formation, *J. Geophys. Res.*, *99*, 6425–6436, doi:10.1029/93JA01501.

Ruohoniemi, J. M., and K. B. Baker (1998), Large-scale imaging of high-latitude convection with Super Dual Auroral Radar Network HF radar observations, *J. Geophys. Res.*, *103*, 20,797–20,811, doi:10.1029/98JA01288.

Russell, C. T., and R. C. Elphic (1978), Initial ISEE magnetometer results: Magnetopause observations, *Space Sci. Rev.*, *22*, 681–715, doi:10.1007/BF00212619.

Sandholt, P., M. Lockwood, T. Oguti, S. Cowley, K. Freeman, B. Lybekk, A. Egeland, and D. Willis (1990), Midday auroral breakup events and related energy and momentum transfer from the magnetosheath, *J. Geophys. Res.*, *95*, 1039–1060, doi:10.1029/JA095iA02p01039.

Sandholt, P. E., J. Moen, A. Rudland, D. Opsvik, W. F. Denig, and T. Hansen (1993), Auroral event sequences at the dayside polar cap boundary for positive and negative IMF B_Y, *J. Geophys. Res.*, *98*, 7737–7755, doi:10.1029/92JA02256.

Smith, C. W., M. H. Acuna, L. F. Burlaga, J. L'Heureux, N. F. Ness, and J. Scheifele (1998), The ACE magnetic fields experiment, *Space Sci. Rev.*, *86*, 613–632, doi:10.1023/A:1005092216668.

Sojka, J. J., M. D. Bowline, R. W. Schunk, D. T. Decker, C. E. Valladares, R. Sheehan, D. N. Anderson, and R. A. Heelis (1993), Modeling polar cap F-region patches using time varying convection, *Geophys. Res. Lett.*, *20*(17), 1783–1786, doi:10.1029/93GL01347.

Valladares, C., S. Basu, J. Buchau, and E. Friis-Christensen (1994), Experimental evidence for the formation and entry of patches into the polar cap, *Radio Sci.*, *29*(1), 167–194, doi:10.1029/93RS01579.

Wannberg, G., et al. (1997), The EISCAT Svalbard radar: A case study in modern incoherent scatter radar system design, *Radio Sci.*, *32*(6), 2283–2307, doi:10.1029/97RS01803.
Weber, E., J. Buchau, J. Moore, J. Sharber, R. Livingston, J. Winningham, and B. Reinisch (1984), *F* layer ionization patches in the polar cap, *J. Geophys. Res.*, *89*, 1683–1694, doi:10.1029/JA089iA03p01683.
Wild, J. A., et al. (2001), First simultaneous observations of flux transfer events at the high-latitude magnetopause by the Cluster spacecraft and pulsed radar signatures in the conjugate ionosphere by the CUTLASS and EISCAT radars, *Ann. Geophys.*, *19*, 1491–1508, doi:10.5194/angeo-19-1491-2001.
Wild, J. A., et al. (2003), Coordinated interhemispheric SuperDARN radar observations of the ionospheric response to flux transfer events observed by the Cluster spacecraft at the high-latitude magnetopause, *Ann. Geophys.*, *21*, 1807–1826, doi:10.5194/angeo-21-1807-2003.
Zhang, Q.-H., et al. (2008), Simultaneous tracking of reconnected flux tubes: Cluster and conjugate SuperDARN observations on 1 April 2004, *Ann. Geophys.*, *26*, 1545–1557, doi:10.5194/angeo-26-1545-2008.
Zhang, Q.-H., et al. (2010), Simultaneous observations of reconnection pulses at Cluster and their effects on the cusp aurora observed at the Chinese Yellow River Station, *J. Geophys. Res.*, *115*, A10237, doi:10.1029/2010JA015526.

M. W. Dunlop and I. W. McCrea, SSTD, Rutherford-Appleton Laboratory, Harwell Science and Innovation Campus, Chilton OX11 0QX, UK.

H.-Q. Hu, Z.-J. Hu, R.-Y. Liu, S.-L. Liu, H.-G. Yang, B.-C. Zhang, and Q.-H. Zhang, Polar Research Institute of China, 451 Jinqiao Rd., Shanghai 200136, China. (zhangqinghe@pric.gov.cn)

M. Lester, Department of Physics and Astronomy, University of Leicester, Leicester LE1 7RH, UK.

M. Lockwood, Space Environment Physics Group, Department of Meteorology, University of Reading, Earley Gate, PO Box 243, Reading RG6 6BB, UK.

J. Moen, Department of Physics, University of Oslo, Oslo N-0316, Norway.